Tellus (1995), 47B, 550–565
Printed in Belgium – all rights reserved

TELLUS
ISSN 0280 6509

Gas diffusivity and production of CO_2 in deep soils of the eastern Amazon

By ERIC A. DAVIDSON[1]* and SUSAN E. TRUMBORE[2], [1]*The Woods Hole Research Center, P.O. Box 296, Woods Hole, MA, 02543, USA*; [2]*Department of Earth System Science, University of California, Irvine, CA, 92717, USA*

(Manuscript received 18 July 1994; in final form 8 February 1995)

ABSTRACT

The rate of gaseous diffusion in soils affects the exchange of gases between the soil and the atmosphere, thereby affecting rates of soil respiration and other soil microbial processes. Understanding the causes of spatial and temporal variation in soil diffusivity will help explain controls of soil sources and sinks of atmospheric gases. In a study of sources of CO_2 in deep soils of forests and pastures of the eastern Amazon, we estimated gaseous diffusivity from bulk density and volumetric water content using published equations that assume the soil to be either an aggregated or nonaggregated medium. The aggregated model requires differentiation of inter- and intra-aggregate pore space; we estimated intra-aggregate pore space from volumetric water content at field capacity. Steady state ^{222}Rn profiles were predicted from a 1-D model using the diffusivities generated by both aggregated and nonaggregated models. Predicted values were compared with ^{222}Rn activities measured to 5 m depth. While the models predict similar radon activities below about 1 m, large differences are predicted for the top 1 m of soil. The non-aggregated model underestimated diffusivity and overestimated ^{222}Rn activities at 1 m and above, which is not surprising given that surface soils are usually well aggregated. Having validated the aggregated media model using the ^{222}Rn profiles, estimates of diffusivity were combined with measured profiles of CO_2 concentrations to estimate CO_2 production by depth. About 70–80% of the measured CO_2 flux from the soil surface was produced in the top 1 m of soil (including litter in the forest). The 20–30% produced below 1 m results from root respiration and microbial decay of root inputs at depth, indicating that deep soil processes are a non-trivial component of carbon cycling in these deep-rooting ecosystems. About 1% of the 20 kg C m^{-2} stock of soil C found between 1 m and 8 m depths turns over annually, indicating that land-use changes that affect rooting depth could significantly affect deep soil C stocks over decades to centuries. Fully understanding the role of land-use change on the global carbon cycle will require consideration of these deep soil processes.

1. Introduction

Because soils store two to three times as much carbon as the atmosphere, the effect of changing climate on soil respiration and other soil microbial processes is important as a potential feedback mechanism of global warming (Billings, 1987; Oechel et al., 1993; Woodwell, 1989). Deforestation and other land-use changes also affect the soil environment and contribute to transfer of C from soils to the atmosphere (Davidson and Ackerman, 1993).

Production of CO_2 by soil microorganisms roughly equals terrestrial net primary productivity (NPP) on a global basis (give or take a couple of gigatons of C per year; Schlesinger, 1991). Above-ground processes such as NPP are more easily studied than are below ground processes such as soil respiration. For example, relatively sophisticated physiological models, based on first-principal understanding of the biochemical mechanisms of plant photosynthesis and respira-

* Corresponding author.

tion, have been developed in so-called "big-leaf" models at local and global scales (Amthor, 1994; Sellers et al., 1992). In contrast, the best soil respiration model may be a simple temperature-dependent Q_{10} function based on empirical fits of data (Raich and Schlesinger, 1992). Soil is difficult to model because it is a complex medium that consists of a broad range of types of organo-mineral particles and aggregates and that contains numerous organisms with differing physiological processes. Soil properties vary temporally and spatially, both horizontally and vertically.

Although the complexity of the soil matrix often seems daunting, some soil processes are understood well enough to make progress towards characterizing probable responses of soils to changes in temperature, precipitation, and land use. One such area of research is the influence of rates of diffusion of gases on soil microbial activity and on fluxes of trace gases such as CO_2, CH_4, N_2O, and NO (Billings, 1987; Davidson, 1993; Born et al., 1990; Oberbauer et al., 1992; Roulet et al., 1992). The presence of O_2 is an important controller of rates of nitrification, denitrification, methane oxidation, methanogenesis, and aerobic respiration (Conrad, 1989; Firestone and Davidson, 1989; Linn and Doran, 1984; Schimel et al., 1993). Understanding the factors that affect diffusion of O_2 into the soil and diffusion of trace gases out of the soil is necessary to describe variation in soil respiration and other soil microbial processes.

The diffusion of gases through soil is dependent on soil porosity and soil water content. Direct measurements of diffusivity of gases in soils are difficult and cumbersome (Dörr and Münnich, 1990; Rolston et al., 1991). Alternatively, gas diffusivity can be calculated from models that require estimates of soil porosity and soil water content. Because it is easier to monitor changes in soil water content than to make frequent direct measurements of effective diffusivity, use of models offers an obvious advantage for studying the dynamics of gas diffusivity in soil.

The models that have been proposed for estimating gas diffusivity range in complexity, data requirements, and usefulness. The most simple models (Millington, 1959; Millington and Quirk, 1961) were intended for nonaggregated media, but have been used, nevertheless, for soils (Hendry et al., 1993; Wood et al., 1993). A model for aggregated media (Millington and Shearer, 1971) is more complicated and requires estimates of inter-aggregate and intra-aggregate porosity and water content. Diffusivity can also be estimated in soils if the distribution of pore sizes can be estimated (Nielson et al., 1984).

The purpose of this research was to develop and test a model of soil gas diffusivity that estimates CO_2 production as a function of depth using only input data on soil profiles of bulk density, CO_2 concentrations, ambient water content, and water content at field capacity. We are interested in CO_2 production deep in the soil because the deeply weathered Oxisols of the eastern Amazon basin contain >20 kg C m^{-2} at depths below 1 m, and roots extend to at least 18 m depth (Nepstad et al., 1994). The turnover time of C in deep soils is not well known, and study of CO_2 production is one means of addressing the dynamics of this deep soil C. We measured profiles of ^{222}Rn, a radioactive noble gas (half-life of 3.8 days) produced in soils by decay of ^{226}Ra, to test models of soil diffusivity. We then applied the model of Millington and Shearer (1971) for aggregated media to measured profiles of CO_2 and water content to show how CO_2 production varies with depth between wet and dry seasons and among forest and pasture sites.

2. Background theory

One of the earliest and most commonly used models of gaseous diffusion in soil (Penman 1940) is a simple linear relation:

$$D_s/D_o = \tau a, \tag{1}$$

where D_s is the diffusion coefficient in soil, D_o is the diffusion coefficient in air (e.g., 0.135 cm^2 s^{-1} for ^{222}Rn and 0.162 cm^2 s^{-1} for CO_2 at 25°C and standard pressure), τ is a dimensionless tortuosity factor, and a is the air-filled porosity (cm^3 air cm^{-3} bed space). Penman (1940) reported a value of 0.66 for τ. However, tortuosity can also be a function of soil water content (Millington, 1959), because the pathway for gaseous diffusion becomes more tortuous as the soil becomes wetter. Hence, τ must be derived for each soil water content of interest for each soil of interest.

Millington (1959) proposed the following relation for diffusion of gases through non-aggregated,

dry, porous media that is assumed to consist of interpenetrating spherical solids separated by interpenetrating spherical pores:

$$D_s/D_o = a^{4/3}. \quad (2)$$

In dry media, a is equivalent to total porosity. As the porosity decreases (due to compaction of a given medium or differences among types of media compared) the probability of pore spaces being continuous declines nonlinearly.

For wet media, the probability of continuous pore spaces declines more rapidly with decreasing air-filled porosity than accounted for in eq. (2). Millington (1959) added a second factor to the equation so that diffusivity is affected not only by the amount of air-filled pore space as in eq. (2), but also by the square of the fraction of total pore space that is air-filled:

$$D_s/D_o = a^{4/3}(a/\varepsilon)^2, \quad (3)$$

where ε is the total porosity (cm^3 pore space cm^{-3} bed space).

In a further refinement of this model, the exponent of the first term of eq. (3) varies to improve the statistical function for the probability of continuity of pore space within the medium (Collin and Rasmuson, 1988; Millington and Quirk, 1961):

$$D_s/D_o = a^{2x}(a/\varepsilon)^2, \quad (4)$$

where x is determined from the relation:

$$a^{2x} + (1-a)^x = 1. \quad (5)$$

The value of x must be solved numerically and typically ranges from 0.6 to 0.8 (Collin and Rasmuson, 1988); $2x$ is usually near 4/3. The value for x can also be approximated from the polynomial:

$$x = 0.477a^3 - 0.596a^2 + 0.437a + 0.564. \quad (6)$$

It is important to note that eqs. (2)–(5) are intended for application to non-aggregated media. Soils are usually aggregated, so it would not be surprising if these equations do not accurately predict diffusion of gases through soils. Millington and Shearer (1971) have proposed a related model for diffusion through aggregated media, but it requires that the soil be conceptually divided into intra-aggregate pore space (ε_{ra}; cm^3 intra-aggregate pore space cm^{-3} bed space) and inter-aggregate pore space (ε_{er}; cm^3 inter-aggregate pore space cm^{-3} bed space). The equation has two terms: the first is for diffusion within the intra-aggregate space, and the second is for diffusion within the inter-aggregate space. The second term is identical to eq. (4), except that the parameters refer specifically to total porosity and air-filled porosity of the inter-aggregate space only:

$$D_s/D_o = \left[\frac{\left(\frac{a_{ra}}{\varepsilon_{ra}}\right)^2\left(\frac{a_{ra}}{\varepsilon_{ra}+S}\right)^{2x}(1-\varepsilon_{er}^{2y})(a_{er}-a_{er}^{2z})}{\left(\frac{a_{ra}}{\varepsilon_{ra}}\right)^2\left(\frac{a_{ra}}{\varepsilon_{ra}+S}\right)^{2x}(1-\varepsilon_{er}^{2y})+(a_{er}-a_{er}^{2z})}\right] + \left[a_{er}^{2z}\left(\frac{a_{er}}{\varepsilon_{er}}\right)^2\right], \quad (7)$$

where a_{ra} is the air-filled intra-aggregate pore space (cm^3 air cm^{-3} bed space), a_{er} is the air-filled inter-aggregate pore space, S is the space occupied by solid (cm^3 solids cm^{-3} bed space), and where x, y, and z are derived from the following equations which are similar to eq. (5):

$$\left(\frac{a_{ra}}{\varepsilon_{ra}+S}\right)^{2x} + \left(1-\frac{a_{ra}}{\varepsilon_{ra}+S}\right)^x = 1, \quad (8)$$

$$\varepsilon_{er}^{2y} + (1-\varepsilon_{er})^y = 1, \quad (9)$$

$$a_{er}^{2z} + (1-a_{er})^z = 1. \quad (10)$$

The length and seemingly complicated nature of eqs. (7)–(10) may discourage some researchers from attempting to use them. More importantly, estimates of intra- and inter-aggregate porosity are often not available. On the other hand, using a model designed for aggregated media, which most soils clearly are, may provide a significant improvement over use of models designed for non-aggregated media, even if only crude estimates of the division between intra- and inter-aggregate porosity are available.

One approach for estimating intra- and inter-aggregate porosities is to assume that all intra-aggregate spaces, and no others, are entirely water-filled at field capacity and, hence, can be estimated from volumetric water content at field capacity (θ_{fc}). Field capacity is defined as "the

content of water, on a mass or volume basis, remaining in a soil 2 or 3 days after having been wetted with water and after free drainage is negligible" (Soil Science Society of America, 1987). The inter-aggregate pore space is assumed to be the macropores that are water-filled only when the soil is saturated, and they are air-filled at field capacity. Hence, inter-aggregate porosity is estimated from the difference between total porosity and volumetric water content at field capacity ($\varepsilon - \theta_{fc}$). Sollins and Radulovich (1988) observed rapid drainage of saturated volcanic soils of Costa Rica until the matric potential reached -0.05 MPa and very slow drainage thereafter. Their soils were highly aggregated, and they deduced that the difference between water content at saturation (when all pore spaces are water-filled) and at field capacity (which they defined as -0.03 MPa for their soils) provided an estimate of the inter-aggregate porosity. Their purpose was to study biphasic flow of water rather than gases, but the same principals should apply to either fluid.

3. Methods

3.1. Site description

The study was conducted at the Fazenda Vitoria (Victory Ranch), located 6.5 km northwest of the town of Paragominas, Pará State, Brazil, in eastern Amazonia (2°59′S, 47°31′W). Paragominas has been a center of cattle ranging and logging since the 1960's (Nepstad et al., 1991). Average annual rainfall is 1750 mm and is highly seasonal; <250 mm fall from July to November in an average year. The forest maintains an evergreen canopy throughout the dry season, apparently by extracting water from deep in the soil profile (Nepstad et al., 1994). The soils are deeply weathered, well-drained, kaolinitic, red-yellow Oxisols (Haplustox). This climate is typical and these soils are common within the "arc of deforestation" ranging from the northeast to the southwest of the Brazilian Amazon (Nepstad et al., 1991). The water table is at about 45 m depth.

3.2. Instrumentation of soil pits

Soil pits were dug by hand in forest and pasture study plots. The pit openings were 1 m × 2 m and they extended to 9 m depth. Three soil pits in forests and three in degraded pasture were studied. To keep illustrative figures from being cluttered, representative data from only one pit per ecosystem type are shown in figures, but data from all pits were used to analyze radon profiles and to calculate depth distribution of CO_2 production.

Pairs of time domain reflectometry (TDR) probes were installed horizontally into the pit wall at 50, 100, 200, 300, 400, 500, 600, 700, and 800 cm depth. Holes (10 cm diameter) were augered 150 cm into the pit walls, the 30 cm long probes were then further inserted into undisturbed soil at the end of the auger holes, and the holes were backfilled. A pair of probes was also installed vertically into the soil surface between 0 and 30 cm depth at each study site. The study sites have been visited weekly for TDR measurements since 1991. The TDR measurements were converted to volumetric water content using calibrations curves derived from laboratory analysis of intact soil cores. The calibration curves are nearly identical to published calibrations of TDR for a variety of other soils (Topp et al., 1980; Topp and Davis, 1985).

Stainless steel tubes (3 mm OD) were also installed horizontally into the pit walls at about 15, 25, 50, 75, 100, 300, 500, and 800 cm depth, and the auger holes (10 cm diameter) were backfilled, except that a chamber about 10 cm long was left open at the far end of the tube buried in the soil. At 100 cm depth and lower, the tubes were 180 cm long. Above 1 m depth the tubes were 90 cm long. Perforations were made in the last 10 cm of tubing to act as inlet vents. The ends protruding from the pit walls were fitted with Swagelok fittings and septa to permit sampling of soil gases with a needle and syringe.

3.3. Measurement of CO_2 flux from the soil surface

Flux measurements were made by circulating air between a LiCor infrared gas analyzer and a flux chamber consisting of a PVC ring (20 cm diameter × 10 cm height) and a vented PVC cover (10 cm height). In the forest, the rings were placed over the forest floor so as not to disturb the litter layer, and wetted soil that is very low in carbon content (taken from deep in the soil pits) was packed around the outside of each ring to maintain a seal; this deep soil produced a small pulse of CO_2 when it was mixed, but CO_2 emissions were negligible after one day, making it suitable for sealing the outside of the chambers. In the pasture

Tellus B/47/5-3

where there is no litter layer, the rings were inserted 1 to 2 cm into the mineral soil. Green plant tissue was clipped prior to placing the cover over each ring. The chamber was vented to the atmosphere through a stainless steel tube (10 cm long × 3.2 mm OD) to keep pressure within the chamber equal to the atmosphere. A battery-operated pump maintained a flow of 0.7 l/min to and from the chamber and the LiCor. Varying the flow rate from 0.4 to 1.2 l/min had no detectable effect on measured flux rates. The LiCor readout was recorded on a 15-s interval with a datalogger and the CO_2 flux was calculated from linear regression of the increasing CO_2 concentrations within the chamber between 1 and 5 min after placing the cover over the ring. 8 flux measurements were taken per site and date; coefficients of variation were typically 30%. The LiCor was calibrated in the field by allowing the pump to draw air from a vented tube through which a standard of 377 ppm CO_2 in air was flowing, while using the same lengths of tubing as in flux measurements to ensure that the LiCor experienced similar pressure differentials during flux measurements and calibrations.

3.4. *Soil CO_2 concentration depth profiles*

The stainless steel tubes inserted into the pit walls were first flushed by removing a 20 ml sample with a syringe and discarding that sample. Duplicate 3 ml samples were then drawn from each tube and the syringes were closed with nylon stopcocks and were carried to the soil surface. A 1 ml sample was then immediately injected from these syringes into a stream of CO_2-free air passing through the LiCor (Fig. 1). The CO_2-free air was produced by filtering air drawn from a battery operated pump through a soda lime scrubber. As the pulse of syringe air drawn from the soil passed through the LiCor, a peak was recorded with a datalogger using 1 s recording intervals. Injections of 0.5 to 3.0 ml of a standard (2.5% CO_2 in air) were also injected to produce a calibration curve relating peak area to CO_2 molar volume. The coefficient of variation for replicate injections of standard gases was usually <2%. The calibration gas concentration was certified to 2%.

To check for the effects of removing large volumes of gas from the soil on the concentration of CO_2 measured, we removed five 20 ml samples from a single gas sampling tube and analyzed a 1 ml subsample from each. After removing a total of 100 ml of soil gas from a single tube, we found no change in CO_2 concentration.

3.5. *Soil radon activity depth profiles*

^{222}Rn measurements were made by direct alpha counting of air samples. Samples of 50 ml were drawn from soil sampling tubes, dried (by passing over a column of Drierite, which is anhydrous calcium sulfate) and introduced into pre-evacuated, 100 ml phosphor-coated Lucas counting cells (Mathieu et al., 1988; Trumbore et al., 1990). Ambient air was used to backfill the cells to atmospheric pressure. The cells were stored for at least 3 hours after filling to establish secular equilibrium of ^{222}Rn with two short-lived, alpha-emitting daughters. Scintillation counting of gross alphas (using a PylonR counter) was performed within 24 h of sample collection. Radon activities were calculated according to the formula:

$$A_{\text{extr}} = \frac{C - B}{\alpha \times \text{CE} \times V \times \exp^{(-\lambda(\text{tmp} - \text{tfc}))}}, \qquad (11)$$

where A_{extr} is the radon activity at the time of sample extraction from the soil; C is the number of counts per minute measured by the counter; B is

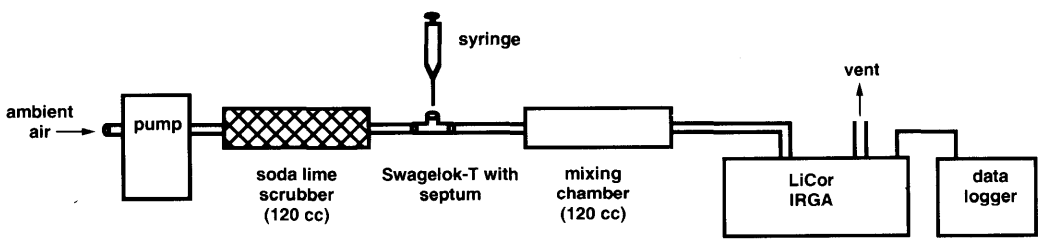

Fig. 1. Diagram of apparatus for field measurement of CO_2 concentrations of syringe samples of soil gases.

Table 1. *Soil properties, volumetric soil water content, and calculated effective diffusivities for CO_2 by depth in a forest and a pasture soil in wet and dry seasons*

	Soil properties					Wet season—May 1992				Dry season—November 1992			
Depth (cm)	total C (%)	bulk density (BD) ($g\ cm^{-3}$)	total porosity (ε) ($cm^3\ cm^{-3}$)	intra-aggregate porosity (ε_{ra}) ($cm^3\ cm^{-3}$)	inter-aggregate porosity (ε_{er}) ($cm^3\ cm^{-3}$)	water-filled porosity (w) ($cm^3\ cm^{-3}$)	air-filled porosity (a) ($cm^3\ cm^{-3}$)	effective diffusivity (D_{eff}); aggregated soil ($cm^2\ s^{-1}$)	effective diffusivity (D_{eff}); non-aggregated soil ($cm^2\ s^{-1}$)	water-filled porosity (w) ($cm^3\ cm^{-3}$)	air-filled porosity (a) ($cm^3\ cm^{-3}$)	effective diffusivity (D_s); aggregated soil ($cm^2\ s^{-1}$)	effective diffusivity (D_s); non-aggregated soil ($cm^2\ s^{-1}$)
Forest Site "C"													
0–30	2.74	0.96	0.63	0.37	0.26	0.29	0.34	0.028	0.011	0.26	0.37	0.029	0.014
30–50	0.90	1.28	0.52	0.37	0.15	0.31	0.21	0.016	0.004	0.34	0.19	0.016	0.003
50–100	0.57	1.28	0.53	0.40	0.13	0.37	0.16	0.013	0.001	0.34	0.19	0.013	0.003
100–200	0.33	1.29	0.53	0.39	0.14	0.37	0.15	0.014	0.001	0.30	0.22	0.014	0.004
200–300	0.26	1.29	0.53	0.38	0.15	0.35	0.18	0.015	0.002	0.26	0.27	0.016	0.007
300–400	0.21	1.30	0.52	0.36	0.16	0.34	0.18	0.017	0.002	0.25	0.28	0.018	0.008
400–500	0.16	1.35	0.51	0.34	0.17	0.29	0.22	0.017	0.004	0.23	0.28	0.018	0.009
500–600	0.12	1.36	0.50	0.33	0.17	0.25	0.25	0.018	0.007	0.22	0.28	0.019	0.009
600–700	0.12	1.36	0.50	0.30	0.20	0.22	0.28	0.022	0.010	0.19	0.31	0.022	0.013
700–800	0.12	1.37	0.50	0.30	0.20	0.26	0.24	0.021	0.006	0.23	0.27	0.021	0.008
Pasture Site "D"													
0–30	2.68	1.21	0.54	0.39	0.15	0.29	0.25	0.015	0.005	0.30	0.24	0.015	0.005
30–50	0.74	1.17	0.57	0.41	0.16	0.34	0.23	0.016	0.004	0.33	0.24	0.016	0.004
50–100	0.45	1.28	0.53	0.40	0.13	0.38	0.15	0.013	0.001	0.30	0.23	0.013	0.005
100–200	0.38	1.29	0.53	0.39	0.14	0.40	0.13	0.011	0.001	0.25	0.27	0.015	0.008
200–300	0.33	1.30	0.52	0.39	0.13	0.36	0.16	0.013	0.002	0.28	0.24	0.014	0.005
300–400	0.25	1.29	0.53	0.41	0.12	0.32	0.21	0.012	0.004	0.32	0.20	0.012	0.003
400–500	0.20	1.29	0.53	0.40	0.13	0.33	0.20	0.013	0.003	0.30	0.23	0.013	0.005
500–600	0.15	1.32	0.52	0.39	0.13	0.32	0.20	0.013	0.003	0.31	0.21	0.013	0.004
600–700	0.15	1.31	0.52	0.39	0.13	0.33	0.19	0.013	0.003	0.31	0.22	0.013	0.004
700–800	0.15	1.26	0.54	0.41	0.13	0.33	0.21	0.013	0.003	0.31	0.23	0.013	0.005

the background when only ambient air is used to fill the cell (5 cpm); α is the factor correcting gross counts to counts due only to decay of ^{222}Rn; CE is the efficiency of the cell-counter combination (cpm for a gas with known radon activity divided by the known activity; cell efficiencies ranged from 64% to 83%, averaging 76% efficient); V is the volume of the soil air sample; and the exponential term corrects for decay of ^{222}Rn ($\lambda = 1.258 \times 10^{-4}$ min^{-1}) in the cell between the time of collection (tfc) and the midpoint of the counting interval (tmp). Calculated errors for radon measurements reflect counting statistics and uncertainties in background and cell efficiency, and were typically about 10% of the measured activity.

3.6. *Laboratory measurements of radon production*

Radon production rates (reported as activity per gram of soil) were measured in the laboratory for both dry and wet soils. First, known quantities (50–100 g) of soil dried to constant weight were sealed in air-tight 100 ml jars. After waiting about 14 days for the ^{222}Rn to come into secular equilibrium with the ^{226}Ra parent, air samples were removed by syringe and the activity of air in the jar was measured. After two or three measurements of the radon production rate from dry soil, distilled water was added to the jars to bring the gravimetric water content to typical field values (16–22% by weight), and measurements were repeated.

3.7. *Calculation of effective diffusivity in soil*

Total porosity (ε) was calculated from measurements of bulk density (BD) and an assumed particle density (PD) of 2.65 g cm^{-3} (Table 1):

$$\varepsilon = 1 - (\mathrm{BD}/\mathrm{PD}). \qquad (12)$$

The mean particle density varies as a function of organic-C content and iron content, but the adjusted values would range only from 2.61 g cm^{-3} for the organic-rich surface soil to 2.73 g cm^{-3} at 5 m depth where maximum total iron content is 5.7% in these soils. Hence, these adjustments of particle density are trivial for calculations of porosity.

Water-filled porosity (w) is simply the volumetric soil water content determined from the calibrated TDR probes (see Subsection 3.2). Air-filled porosity is the difference between total porosity and water-filled porosity ($\varepsilon - w$; Table 1). For calculation of effective diffusivity in soil (D_s) using the nonaggregated model for dry media (eq. (2)), only air-filled porosity (a) is needed. For calculation of D_s using the nonaggregated model for wet media (eq. (4)), only total porosity (ε) and air-filled porosity (a) are needed.

To use the aggregated soil model of eq. (7), the pore spaces must be partitioned into intra- and inter-aggregate spaces. Intra-aggregate porosity was estimated from volumetric soil water content at field capacity, which was measured by TDR probes about 48 h after a soaking rain near the end of the wet season in 1991. Field capacity is often estimated from water content measured at either −0.01 MPa or −0.03 MPa tension in the laboratory, but field capacity is more appropriately defined as the water content after a saturated soil has drained freely (Soil Science Society of America, 1987), which can result in a matric potential between −0.01 and −0.03 MPa, depending on soil texture (Papendick and Campbell, 1981). Our in situ estimates of field capacity happened to agree reasonably well with laboratory estimates at −0.03 MPa tension, but no specific matric potential for field capacity is assumed, and this approach conforms more closely to the formal definition of field capacity. It is assumed that, 48 h after rainfall has elevated the soil water content above field capacity, water has drained from the inter-aggregate pore spaces, leaving the intra-aggregate pore spaces 100% water-filled ($\varepsilon_{ra} = \theta_{fc}$). Inter-aggregate porosity (ε_{er}) is estimated from the difference between total porosity and intra-aggregate porosity ($\varepsilon_{er} = \varepsilon - \varepsilon_{ra}$; Table 1). For calculating diffusivity, it is assumed that the intra-aggregate spaces store water first and lose water last. When $w \leqslant \varepsilon_{ra}$, ε_{er} is entirely air-filled so that $a_{er} = \varepsilon_{er}$ and $a_{ra} = \varepsilon_{ra} - w$. When $w > \varepsilon_{ra}$, $a_{ra} = 0$ and $a_{er} = \varepsilon - w$.

4. Results and discussion

4.1. *Radon profiles and estimates of diffusivity*

Activities of ^{222}Rn increased sharply from the surface to 1 m depth and then remained relatively constant from 1 m depth downward (Fig. 2). Depth profiles of ^{222}Rn such as these have been fitted to exponential equations to estimate diffusivity

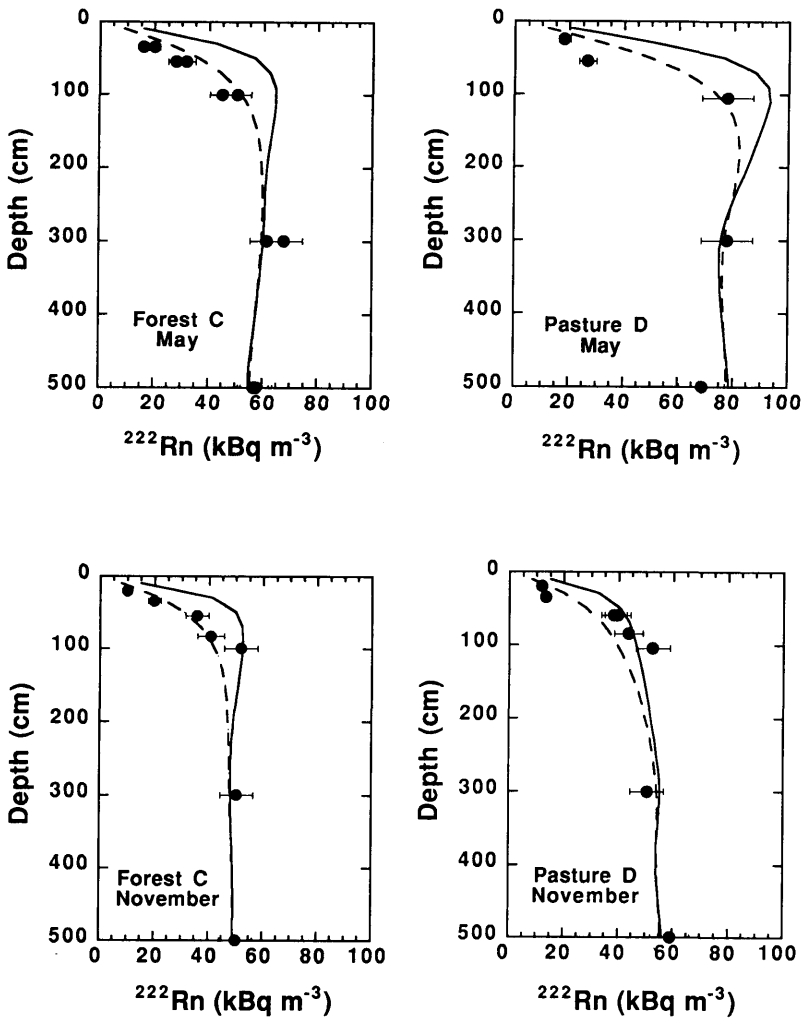

Fig. 2. Depth profiles of radon activities in one forest soil and one pasture soil near the end of the wet season (May 1992) and near the end of the dry season (November 1992). Circles show duplicate measured values, and error bars represent uncertainty due to analytical error (cell counting efficiencies, etc.). The solid lines show the predicted values using the nonaggregated model (eq. (4)), and the broken lines show the predicted values using the aggregated soil model (eq. (7)).

(Dörr and Münnich, 1990), but this approach assumes constant diffusivity with depth. Significant gradients of soil water content in the upper two meters of the soil indicate that uniform diffusivity is unlikely, and calculated diffusivities from both aggregated and non-aggregated models support this conclusion (Table 1). In addition, ^{222}Rn activity (concentration) gradients in the upper part of the soil also depend on the radon activity at depth. Variations in the amount of air-filled versus water-filled pore space can cause significant changes in the observed deep soil radon activity on a seasonal timescale (Asher-Bolinder et al., 1990; Washington and Rose, 1990). To account for these non-ideal conditions, we used a multi-box model that predicts ^{222}Rn activities

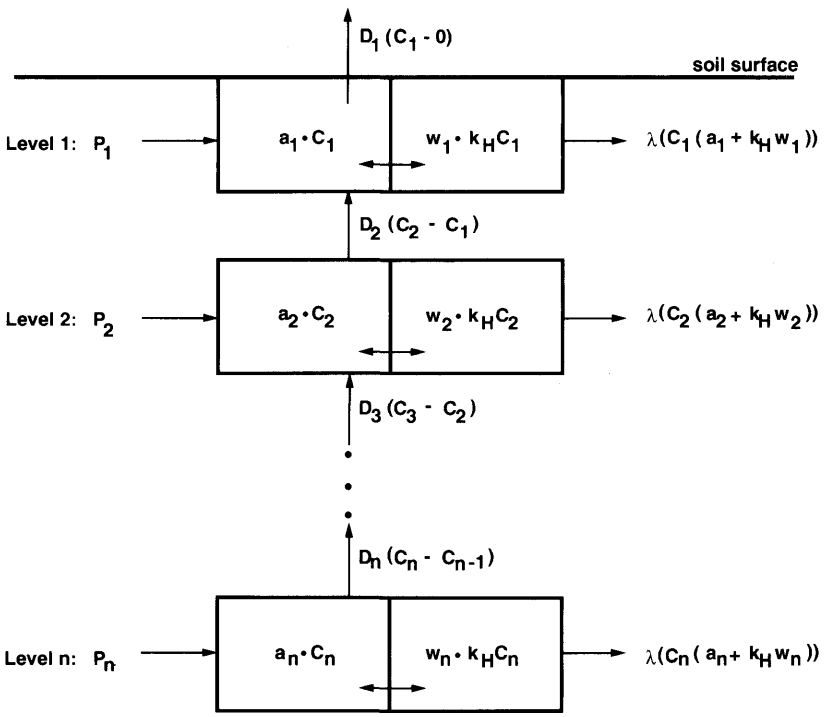

Fig. 3. Diagram of model used for predicting depth profiles of radon activities and CO_2 production, where a is the air phase, w is the water phase, C is concentration (or activity of radon) in the air phase, D is diffusivity, k_H is the Bunsen coefficient, λ is the decay constant for ^{222}Rn, and P is the radon production rate. The soil is divided into 50 layers, each of 10 cm depth.

throughout the soil profile using estimates of radon production and diffusion, and we compared these predictions with measured ^{222}Rn activities.

To predict steady state radon activities in the soil atmosphere, we used the model illustrated in Fig. 3. The soil is divided into boxes (layers) of 10-cm depth, and the balance of radon is calculated through successive iterations using a 10 minute time step until steady state is reached, usually in two weeks (4 half-lives of ^{222}Rn):

$$\begin{aligned} d(\mathrm{TotRn}_i)/dt = {} & P_i - \lambda(\mathrm{TotRn}_i) \\ & + D_{i-1}(\mathrm{airRn}_{i-1} - \mathrm{airRn}_i) \\ & - D_i(\mathrm{airRn}_i - \mathrm{airRn}_{i+1}), \end{aligned} \quad (13)$$

where for layer i, TotRn_i is total ^{222}Rn (including air and water phases), airRn_i is the ^{222}Rn activity in soil air, P_i is ^{222}Rn production, D_i is diffusivity.

Production of ^{222}Rn was estimated in two ways: (i) the laboratory jar incubations described in Subsection 3.6; and (ii) by back-calculation of radon production from in situ radon activities in the deep (>3 m) soil. In the laboratory jar method, dry soil radon production rates varied by depth, decreasing rapidly from values of 13.5 Bq kg^{-1} (range: 9.5 to 17.0 Bq kg^{-1}) in the top 10 cm of soil to an average of 4.5 Bq kg^{-1} (range: 2.7 to 8.8 Bq kg^{-1}) for depths of 50 to 800 cm. The radon production rates were higher in wet soil, as has been observed by others (Stranden et al., 1984; Strong and Levins, 1982), with a mean of 19.3 Bq kg^{-1} for the top 10 cm, and a mean of 8.3 Bq kg^{-1} (range: 4.5 to 11.7 Bq kg^{-1}) for depths greater than 50 cm.

For the method based on calculations of measured in situ radon activities of deep soil, the

production rate (P) (Bq kg^{-1} soil) was calculated from the formula:

$$A = P \times BD \times \frac{1}{a + 0.22w}, \quad (14)$$

where A is radon activity (kBq m^{-3} air-filled pore space) for a given volume of soil; BD is the bulk density (g soil cm^{-3} bed space), a the air-filled pore space (cm^3 air cm^{-3} bed space) and w is the water-filled pore space (cm^3 water cm^{-3} bed space), and the Henry's Law constant for ^{222}Rn is 0.22 (assuming instantaneous equilibration between air and water). This calculation is based on the assumption that the radon in the deep (>3 m) soil is in secular equilibrium with the ^{226}Ra parent, which appears reasonable for soils below 2 m. Given a typical effective diffusivity of 0.015 $cm^2\ s^{-1}$, the time required for radon to diffuse from 3 m to the surface is approximately 70 days (square of the distance divided by the effective diffusivity), which is much longer than the half-life of ^{222}Rn (3.8 days). Hence, the equilibrium activity at depth is determined primarily by production and decay of ^{222}Rn, and not by loss to the surface. The only reason the deep soil radon content would not be at equilibrium would be if there were significant lateral exchange through the pit wall. The time required to diffuse the 1.7 m length of the sampling tubes would be about 25 days, again indicating that most of the radon would decay before escaping the soil via the pit wall. Analytical errors in the range of 10% of measured ^{222}Rn activities are greater than errors resulting from the influence of the pit wall.

Radon production for deep soils calculated from eq. (14) averaged 12 Bq kg^{-1} in forests for both wet and dry seasons and averaged 16 Bq kg^{-1} in the pastures in the wet season and 12 Bq kg^{-1} in the dry season. These values are greater than production measured in either wet or dry jar incubations. We attribute this to the tendency of the wetted soils in the incubation jars to form clumps, which may have trapped radon within the soil. Thus, for most of the soil profile we chose to calculate the average radon production rates by the second method, which assumes equilibrium at depth. Radon production rates cannot be calculated from in situ measurements in the upper two meters of the soil, however, as these depths are affected by diffusive loss of radon to the overlying air in addition to radioactive decay. The jar incubation data clearly show that radon production rates in the top 50 cm of the soil are greater than those below, probably because radium is taken up by plants due to its similarity with other divalent cation nutrient elements and is concentrated in the plants and plant detritus. We therefore used the wet jar incubation value (19 Bq kg^{-1}) for the surface soil layer, and assumed a linear decrease to 50 cm, at which point the average deep in situ value (12 or 16 Bq kg^{-1}, depending on the site and season) was assumed to be constant to 500 cm depth. Model results are not sensitive to changing the surface value by 60%.

Seasonal variation in measured radon activities in forest soils (Fig. 2) can be explained using eq. (14) by the differences in water-filled porosity between wet and dry season and by assuming no change in production rate. In other words, a simple dilution effect caused by expansion and contraction of the air volume within the soil significantly affects the secular equilibrium value of radon activity when radon production is constant. Hence, variation in rates of radon production need not be invoked in this case to account for observed changes in radon activities. Larger seasonal changes in radon activities of pasture soils, however, require higher production rates to explain the high wet season deep soil radon activities. As we and others have observed in laboratory incubations (Stranden et al., 1984; Strong and Levins, 1982), radon production in soils is positively related to water content in soils, presumably due to reduced adsorption of radon onto surface particles when the surfaces are wet and because the soil water increases the emanation coefficient of radon. The ^{222}Rn generated by alpha-decay of ^{226}Ra possesses kinetic energy (alpha recoil energy), which is dissipated as the ^{222}Rn atom moves away from the site at which it was generated. In a fine grained medium, this distance may be great enough to transport the ^{222}Rn across air-filled pore spaces and into the next mineral grain. The presence of water in pore spaces serves to decrease the recoil range markedly, thus trapping the recoiled ^{222}Rn in pore spaces, and increasing the radon emanation observed in wet soils compared to dry soils (Nazaroff, 1992). The pasture soil was very wet at depth in the wet season (Table 1), and perhaps these extreme conditions

are needed for the water effect on radon production rates to be detectable by our in situ measurements.

Returning to the model illustrated in Fig. 3, the soil properties shown in Table 1 were linearly interpolated between measured or calculated values to provide estimates for each 10 cm soil layer. Diffusivity was estimated for each soil layer using eq. (4) for the nonaggregated soil model and eq. (7) for aggregated soil model. Total radon in each 10-cm soil layer was distributed among air and dissolved phases using the Henry's law constant of 0.22 at 25°C in fresh water (eq. (14)). We assumed instantaneous equilibration between soil air and water, that advective losses of radon were insignificant, and that diffusion gradients were based solely on activity (concentration) gradients in the soil air. The bottom soil box was assumed to have constant activity (equal to its secular equilibrium value). Predicted profiles of ^{222}Rn from the nonaggregated and aggregated models as well as observed ^{222}Rn activities are shown in Fig. 2.

The choice between nonaggregated and aggregated soil models has no effect on modeled equilibrium activities of ^{222}Rn at depth (Fig. 2). As discussed above, the activity at depth is influenced primarily by rates of production and by the changing proportions of water-filled and air-filled pore space, rather than by diffusive losses to the surface or the pit wall. In contrast, the choice of diffusivity equations is important near the soil surface. The nonaggregated model significantly underestimates diffusivity in the top 1 m of soil, and this model predicts higher radon activities than were observed, including a large bulge in ^{222}Rn in the top 1 m of soil (Fig. 2). This failure of the nonaggregated model is not surprising, given that soils are aggregated media. Diffusivities calculated from the non-aggregated model are between 2 and 10 times lower that those from the aggregated model (Table 1). The aggregated soil model predicts ^{222}Rn activities that agree well with observed activities throughout the profile (Fig. 2). We concluded that the aggregated model of eq. (7) (Millington and Shearer, 1971) works well for these soils and we adopted it for subsequent analyses of CO_2 production.

4.2. *Simplification of the aggregated media diffusivity model*

The disadvantages of the aggregated media model of Millington and Shearer (1971) are its seemingly complicated structure and its requirement for differentiating among inter- and intra-aggregate porosity (eq. (7)). We have shown that the later can be overcome if data are available on volumetric water content at field capacity and if it is assumed that intra-aggregate spaces are water-filled and inter-aggregate spaces are air-filled at field capacity.

Eqs. (7)–(10) are not as difficult to work with as first impressions may indicate. Nevertheless, we have noted that the imposing nature of the aggregated media model could be mitigated by a simplification that is possible for the soils of this study and may be applicable elsewhere. The first term of eq. (7) accounts for diffusion through intra-aggregate pore spaces, but in all of the cases we applied it (all soil pits, all dates, and all depths), this term never accounted for more that 7% of the effective diffusivity and usually only accounted for 1% or 2%. Hence, the first term could be dropped with little effect on the calculation of diffusivity, leaving the simplified formula:

$$D_s/D_o = a_{er}^{2z}(a_{er}/\varepsilon_{er})^2. \quad (15)$$

It is likely that this simplified formula would perform satisfactorily in fine textured soils where water is often held tenaciously in small intra-aggregate pore spaces. The difference in volumetric water content, and hence in intra-aggregate air-filled pore space, between soils at field capacity and at -1.5 MPa matric potential is relatively small in fine textured soils. This simplified formula would be less likely to work in coarse textured soils, where the proportional change in water content is greater, but it deserves testing.

Whether the full model or the simplified version is used, the aggregated media model is more appropriate for use in soils, especially in surface soils, than are other models. Gaseous diffusivity in soil can be estimated using only data on bulk density and water content at field capacity to characterize the soil and data on volumetric water content to account for the dynamics.

4.3. *CO_2 profiles and estimates of CO_2 production by depth*

Unlike ^{222}Rn, CO_2 does not decay, and the precision of our CO_2 concentration estimates is $<2\%$, which is superior to the precision of the ^{222}Rn measurements. Hence, the effect of mixing

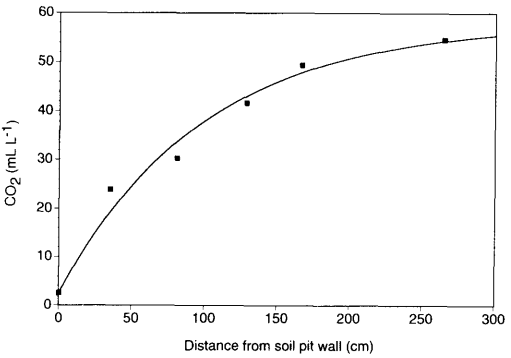

Fig. 4. Horizontal profiles of CO_2 concentrations from the soil pit wall inward at 5 m depth in a forest soil measured early in the dry season (August 1993). The line shows the regression equation:

$$CO_{2(z)} = CO_{2(\infty)}(1 - e^{(-az)}) + 2.5,$$

where z is the tubing length (cm), $CO_{2(\infty)}$ is a fitted parameter for the asymptote CO_2 concentration (55.5 ml CO_2 l^{-1} air), a is a fitted exponential parameter, and 2.5 ml CO_2 l^{-2} air is the measured CO_2 concentration in the air of the soil pit.

of air from within the soil pit with air sampled near the end of the 180-cm long tubes is potentially within the range of detection of our CO_2 measurements. Ideally, the tubes would be sufficiently long to avoid the pit wall effect for all gases, but this was not feasible because the longest dimension of the pit is only 180 cm, and an extension had to be taken on and off the auger for each auger bucket of soil removed beyond 180 cm. To test the effect of the pit wall on measured CO_2 concentrations, we inserted tubes of 45, 90, 135, 180, and 270 cm length horizontally into the side of one of the forest soil pits at 5 m depth. An exponential fit of the horizontal CO_2 concentration gradient measured in August, 1993, early in the dry season, is shown in Fig. 4. The estimated asymptote concentration at infinite tubing length from an exponential nonlinear fit is 58 ml CO_2 l^{-1} soil air. The CO_2 concentration measured at 170 cm from the pit wall (about 10 cm of the 180 cm tube extends out into the pit) was 49 ml CO_2 l^{-1} soil air, or 85% of the concentration at the asymptote.

This correction factor can also be independently estimated from estimates of diffusivity and using ^{222}Rn as a proxy for CO_2. We cannot use CO_2 profiles directly because the equilibrium concentration of CO_2 is determined by production and diffusion, both of which are unknown. As already discussed, the ^{222}Rn concentration at equilibrium is determined by the rate of production and decay, and the decay rate of ^{222}Rn is known. The quotient of the ^{222}Rn activity at a given distance from the pit wall ($^{222}Rn_z$) divided by the ^{222}Rn activity at an infinite distance ($^{222}Rn_\infty$), where production and decay are at equilibrium, can be calculated from the exponential function described by Dörr and Münnich (1990):

$$\frac{[^{222}Rn]_z}{[^{222}Rn]_\infty} = (1 - e^{-kz}), \qquad (16)$$

where z is the distance from the pit wall in cm, $k = \sqrt{(\lambda/D_s)}$, λ is the decay constant for ^{222}Rn (2.0978×10^{-6} s^{-1}), and D_s is the effective diffusivity of ^{222}Rn in soil calculated from eq. (7). Constant diffusivity and constant ^{222}Rn production along the horizontal length of the sampling tube are assumed. This quotient must then be multiplied by 1.2 to account for more rapid diffusion of CO_2 relative to ^{222}Rn. The quotient from eq. (16), adjusted for CO_2, is 0.85 for 170 cm distance from the pit wall at 5 m depth and measured soil water contents of August, 1993, and using the diffusivity estimates from the aggregated media model (eq. (7)). The excellent agreement between the quotient calculated from diffusivity estimates and the correction factor estimated from the measured horizontal CO_2 profile shown in Fig. 4 indicates that the aggregated media model yields reasonable estimates and that the measured CO_2 concentrations within the deep soil can be reliably adjusted to account for diffusional losses through the pit walls. The quotients calculated from eq. (16) ranged from 0.80 to 0.95 for the data from our 6 soil pits in pastures and forests and during wet and dry seasons.

Depth profiles of measured concentrations of CO_2 (not corrected for the pit wall effect) are shown in Fig. 5, and they increased with depth to at least 8 m. Concentrations at depth are higher in forest soils than in pasture soils. Concentration alone, however, does not indicate the strength of CO_2 production sources, because high concentrations can result from either high rates of production or low rates of diffusion.

To estimate CO_2 production, we first solved eq. (16) for the asymptote CO_2 concentration at

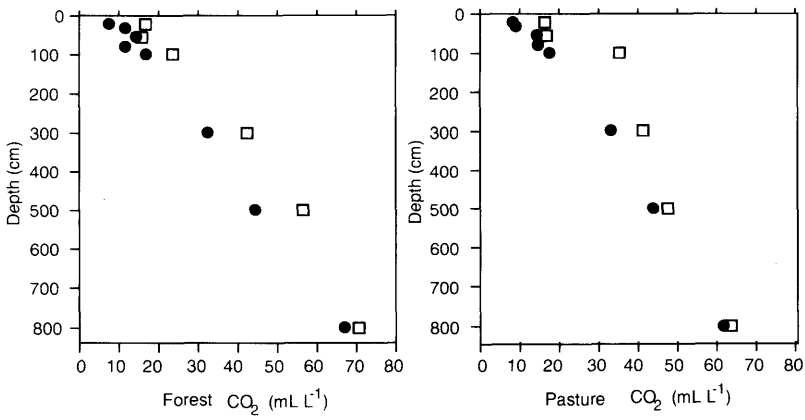

Fig. 5. Depth profiles of CO_2 concentration (means of duplicate analyses) in forest and pasture during the wet season (squares) and the dry season (circles). Data are from the same sites and dates as shown for radon activities in Fig. 2.

infinite tube length, using estimates of diffusivity from the aggregated media model (eq. (7)) and measured concentrations at 170 cm tube length at depths below 1 m. We then applied the corrected CO_2 concentration profiles and the diffusivity estimates to a model based on Fick's first law. The CO_2 production ($P_{CO_2,i}$) within each 10-cm soil layer of the model represented by Fig. 3 was estimated from the difference between the CO_2 flux calculated from Fick's first law at the top and bottom of each layer:

$$P_{CO_2,i} = [D_i \times (C_i - C_{i-1})/z] - [D_{i+1} \times (C_{i+1} - C_i)/z] \quad (17)$$

where for layer i, D_i is the diffusivity calculated for the aggregated medium model (eq. (7)), C_i is the soil CO_2 concentration, z and is the depth increment (10 cm). Concentrations of CO_2 were linearly interpolated to estimate CO_2 concentrations within each 10 cm layer. Because of uncertainties in interpolations of CO_2 concentrations and soil water contents, the CO_2 production estimates for individual 10 cm layers may not be reliable, but reliability increases as estimates from the 10 cm layers are summed for larger depth increments that include measured values of input variables. We also suspect that this approach underestimates CO_2 production in the layers above 1 m, because CO_2 concentrations are not linear or unimodal in this region, but rather exhibit "hot spots" of high CO_2 production and concentration. Finally, CO_2 production in the forest floor litter cannot be estimated directly by eq. (17) because we do not have estimates of diffusivity or measurements of CO_2 concentration in the forest floor layer.

The ecological question of interest is the relative importance of surface and deep soils as sources of soil CO_2 in forests and pastures. For this purpose, we have grouped the production estimates for three large depth intervals (Table 2). Production below 5 m is simply the flux calculated from Fick's first law at 5 m depth—any CO_2 diffusing upward at that depth is assumed to have been produced below. Production below 5 m depth may be underestimated if there is also a downward flux of CO_2 at some depth, either through the soil atmosphere or dissolved in drainage water. We cannot address at this time the magnitude of export of CO_2 via the groundwater. The production estimate for the 1 to 5 m depth increment is the sum of the CO_2 production rates calculated from eq. (17) for all of the 10 cm soil layers between 1 and 5 m. The estimate for the litter layer plus the top 1 m of mineral soil is the difference between measured fluxes of CO_2 from the soil/litter surface (Subsection 3.3, Table 2), and the Fick's law flux calculated at 1 m. These estimates were calculated for each of the three soil pits in forest and pasture, and the means are reported in Table 2.

Surface fluxes of CO_2 from the forest are about twice the rates measured in the degraded pastures (Table 2). The forests are more productive eco-

Table 2. *Summary of measured CO_2 fluxes from the soil surface and calculated rates of production of CO_2 by depth increments within the soil and litter (L); means (rounded to the nearest 10 mg) and standard errors are of three soil pits per ecosystem type*

	Wet season (May 1992)				Dry season (November 1992)			
	forest		pasture		forest		pasture	
	mean	SD	mean	SD	mean	SD	mean	SD
	mg CO_2-C m^{-2} h^{-1}							
surface flux	290	20	140	6	240	20	110	23
production: L to 1 m	240	24	100	16	200	26	70	26
production: 1 to 5 m	30	5	30	11	10	15	20	4
production: below 5 m	20	7	<10	2	30	15	10	0

systems than are degraded pastures, and below-ground inputs of C are apparently higher in the forests than in the pastures. About 70–80% of the production in both ecosystems occurs within the top 1 m of soil, including the forest litter layer. Very little CO_2 (≤ 10 mg C m^{-2} hr^{-1}) is produced below 5 m depth in the pasture. Production of CO_2 below 5 m depth is also low in the forest sites relative to the surface, but the deep soil CO_2 production rates in forests are more than double those in the pastures.

4.4. Ecological significance of research findings

The deep roots of eastern Amazonian forests enable the vegetation to extract water stored deep in the soil and thus retain green foliage during the long dry season (Nepstad et al., 1994). In contrast, pasture vegetation turns brown during the dry season and pasture vegetation extracts less water from deep soils. Active extraction of soil water by deep forest roots must be accompanied by root respiration and microbial decomposition of root inputs and by concomitant production of CO_2. Although most of the CO_2 production is concentrated in the top 1 m of soil, as are most of the roots (Nepstad et al., 1994), the deep soil processes are not trivial. Our estimates of CO_2 production by depth (Table 2) are consistent with the depth distribution of fine root biomass reported by Nepstad et al. (1994), in which 70% to 80% occurred above 1 m and the remainder below 1 m depth. Changes in land use, from deep-rooted forest vegetation to more shallowly rooted pasture vegetation, could change the depth distribution of root biomass, CO_2 production, and the dynamics of soil organic matter. If half of the CO_2 produced below 1 m depth emanates from microbial decomposition (the other half emanating from root respiration), the annual rate of microbial decomposition of soil organic matter below 1 m depth would be about 0.2 kg C m^{-2}, which indicates that, on average, about 1% of 20 kg C m^{-2} stock of soil C found between 1 m and 8 m depths turns over annually. If C inputs to deep soils decline when forests are converted to pastures, the deep soil C stocks could change significantly over decades to centuries. Fully understanding the role of land use change on the global carbon cycle will require consideration of these deep soil processes.

5. Acknowledgements

This study was funded by NASA grants NAGW-2750, NAGW-2748, and NAGW-3748. The authors thank the director and staff of the Empresa Brasileira de Pesquisa Agropecuária/ Centro de Pesquisa Agropecuária do Trópico Umido (EMBRAPA/CPATU) for logistical support. We thank Daniel C. Nepstad and Peter H. Jipp for use of their TDR data, for making available the research site infrastructure that they developed, and for their generous assistance, without which this research would not have been possible. We also thank Michael Keller, Daniel Nepstad, Eric Sundquist, and two anonymous reviewers for helpful comments on earlier drafts of this manuscript.

REFERENCES

Asher-Bolinder, S., Owen, D. E. and Schmann, R. R. 1990. Pedologic and climatic controls on Rn-222 concentrations in soil gas. *Geophys. Res. Lett.* **17**, 825–828.

Amthor, J. S. 1994. Scaling CO_2-photosynthesis relationships from the leaf to the canopy. *Photosynthesis Res.* **39**, 321–350.

Billings, W. D. 1987. Carbon balance of Alaskan tundra and taiga ecosystems: past, present, and future. *Quat. Sci. Rev.* **6**, 165–177.

Born, M., Dörr, H. A. and Levin, I. 1990. Methane consumption in aerated soils of the temperate zone. *Tellus* **42B**, 2–8.

Collin, M. and Rasmuson, A. 1988. A comparison of gas diffusivity models for unsaturated porous media. *Soil Sci. Soc. Am. J.* **52**, 1559–1565.

Conrad, R. 1989. Control of methane production in terrestrial ecosystems. In: *Exchange of trace gases between terrestrial ecosystems and the atmosphere* (eds. M. O. Andreae and D. S. Schimel). John Wiley & Sons Publishers, New York, 39–58.

Davidson, E. A. and Ackerman, I. L. 1993. Changes in soil carbon inventories following cultivation of previously untilled soils. *Biogeochem.* **20**, 161–193.

Davidson, E. A. 1993. Soil water content and the ratio of nitrous oxide to nitric oxide emitted from soil. In: *The biogeochemistry of global change* (ed. R. S. Oremland). Chapman and Hall Publishers, New York, 369–386.

Dörr, H. and Münnich, K. O. 1990. ^{222}Rn flux and soil air concentration profiles in West-Germany. Soil ^{222}Rn as tracer for gas transport in the unsaturated soil zone. *Tellus* **42B**, 20–28.

Firestone, M. K. and Davidson, E. A. 1989. Microbiological basis of NO and N_2O production and consumption in soil. In: *Exchange of trace gases between terrestrial ecosystems and the atmosphere* (eds. M. O. Andreae and D. S. Schimel). John Wiley & Sons Publishers, New York, 7–21.

Hendry, M. J., Lawrence, J. R., Zanyk, B. N. and Kirkland, R. 1993. Microbial production of CO_2 in unsaturated geologic media in a mesoscale model. *Water Resour. Res.* **29**, 973–984.

Linn, D. M. and Doran, J. W. 1984. Effect of water-filled pore space on carbon dioxide and nitrous oxide production in tilled and nontilled soils. *Soil Sci. Soc. Am. J.* **48**, 1267–1272.

Mathieu, G. G., Biscaye, P. E., Lupton, R. A. and Hammond, D. E. 1988. System for measurement of ^{222}Rn at low levels in natural waters. *Health Physics* **55**, 989–992.

Millington, R. J. 1959. Gas diffusion in porous media. *Science* **130**, 100–102.

Millington, R. J. and Quirk, J. P. 1961. Permeability of Porous Solids. *Trans. Farad. Soc.* **57**, 1200–1207.

Millington, R. J. and Shearer, R. C. 1971. Diffusion in aggregated porous media. *Soil Sci.* **3**, 372–378.

Nazaroff, W. W. 1992. Radon transport from soil to air. *Reviews of Geophysics* **30**, 137–160.

Nepstad, D. C., Carvalho, C. R. de., Davidson, E. A., Jipp, P. H., Lefebvre, P. A., Negreiros, G. H., Silva, E. D. de., Stone, T. A., Trumbore, S. E. and Vieira, S. 1994. The deep-soil link between water and carbon cycles of Amazonian forests and pastures. *Nature* **372**, 666–669.

Nepstad, D. C., Uhl, C. and Serrao, E. A. S. 1991. Recuperation of a degraded Amazonian landscape: forest recovery and agricultural restoration. *Ambio* **20**, 248–255.

Nielson, K. K., Rogers, V. C. and Gee, G. W. 1984. Diffusion of radon through soils: a pore distribution model. *Soil Science Society of America Journal* **48**, 482–487.

Oberbauer, S. F., Gillespie, C. T., Cheng, W., Gebauer, R., Sala Serra, A. and Tenhunen, J. D. 1992. Environmental effects on CO_2 efflux from riparian tundra in the northern foothills of the Brooks Range, Alaska, USA. *Oecologia* **92**, 568–577.

Oechel, W. C., Hastings, S. J., Vourlitis, G., Jenkins, M., Riechers, G. and Grulke, N. 1993. Recent change of Arctic tundra ecosystems from a net carbon dioxide sink to a source. *Nature* **361**, 520–523.

Papendick, R. I. and Campbell, G. S. 1981. Theory and measurement of water potential. In: *Water potential relations in soil microbiology* (ed. J. F. Parr et al.). ASA Spec. Publ. No. 9, Agronomy Society of America Publishers, Madison, Wisconsin, 1–22.

Penman, H. L. 1940. Gas and vapor movements in the soil (I). The diffusion of vapors through porous solids. *J. Agr. Sci.* **30**, 437–461.

Raich, J. W. and Schlesinger, W. H. 1992. The global carbon dioxide flux in soil respiration and its relationship to climate. *Tellus* **44B**, 81–99.

Rolston, D. E., Glauz, R. D., Grundmann, G. L. and Louie, D. T. 1991. Evaluation of an in situ method for measurement of gas diffusivity in surface soils. *Soil Sci. Soc. Am. J.* **55**, 1536–1542.

Roulet, N. T., Ash, R. and Moore, T. R. 1992. Low boreal wetlands as a source of atmospheric methane. *J. Geophysical Res.* **97**, 3739–3749.

Schimel, J. P., Holland, E. A. and Valentine, D. 1993. Controls on methane flux from terrestrial ecosystems. In: *Agricultural ecosystem effects on trace gases and global climate change* (ed. L. A. Harper et al.). ASA Spec. Publ. No. 55, Agronomy Society of America, Madison, Wisconsin, 167–182.

Schlesinger, W. H. 1991. *Biogeochemistry: an analysis of global change.* Academic Press Publishers, New York.

Sellers, P. J., Berry, J. A., Collatz, G. J., Field, C. B. and Hall, F. G. 1992. Canopy reflectance, photosynthesis, and transpiration (III). A reanalysis using improved leaf models and a new canopy integration scheme. *Remote Sens. Environ.* **42**, 187–216.

Soil Science Society of America. 1987. Glossary of soil science terms. Soil Science Society of America, Madison, Wisconsin.

Sollins, P. and Radulovich, P. 1988. Effects of soil physical structure on solute transport in a weathered tropical soil. *Soil Sci. Soc. Am. J.* **52**, 1168–1173.

Stranden, E., Kolstad, A. K. and Lind, B. 1984. The influence of moisture and temperature on radon exhalation. *Radiat. Prot. Dosim.* **7**, 55–88.

Strong, K. P. and Levins, D. M. 1982. Effect of moisture content on radon emanation from uranium ore and tailings. *Health Physics* **42**, 27–32.

Topp, G. C., Davis, J. L. and Annan, A. P. 1980. Electromagnetic determination of soil water content: Measurements in coaxial transmission lines. *Water Resour. Res.* **16**, 574–582.

Topp, G. C. and Davis, J. L. 1985. Measurement of soil water content using time domain reflectometry (TDR): A field evaluation. *Soil Sci. Soc. Am. J.* **49**, 19–24.

Trumbore, S. E., Bonani, G. and Wölfli, W. 1990. The rates of carbon cycling in several soils from AMS ^{14}C measurements of fractionated soil organic matter. In: *Soils and the greenhouse effect* (ed. A. F. Bouwman). John Wiley Publishers, New York, 405–414.

Washington, J. W. and Rose, A. W. 1990. Regional and temporal relations of radon in soil gas to soil temperature and moisture. *Geophys. Res. Lett.* **17**, 829–832.

Wood, B. D., Keller, C. K. and Johnstone, D. L. 1993. In situ measurement of microbial activity and controls on microbial CO_2 production in the unsaturated zone. *Water Resour. Res.* **29**, 647–659.

Woodwell, G. M. 1989. The warming of the industrialized middle latitudes 1985–2050: causes and consequences. *Climatic Change* **15**, 31–50.